JOURNAL OF CATALYSIS 82, 341–350 (1983)

Structure Sensitivity in Methanol Decomposition on ZnO Single-Crystal Surfaces

W. H. CHENG,[1] S. AKHTER, AND H. H. KUNG[2]

Department of Chemical Engineering, Ipatieff Laboratory, and the Materials Research Center, Northwestern University, Evanston, Illinois 60201

Received June 9, 1982; revised February 28, 1983

Decomposition of methanol-d_4 was studied using temperature-programmed decomposition spectroscopy on the nonpolar flat $(10\bar{1}0)$, stepped $(50\bar{5}1)$ and $(40\bar{4}1)$, and the polar (0001) ZnO surfaces. The $(50\bar{5}1)$ and $(40\bar{4}1)$ planes are surfaces with (0001) steps and $(10\bar{1}0)$ terraces. CD_4, CO, CO_2, and D_2 were the decomposition products on the nonpolar stepped and flat surfaces. The ratios of these products were similar on these surfaces. The fraction of desorbed product being decomposition products increased in the order stoichiometric $(10\bar{1}0)$ < reduced $(10\bar{1}0)$ < $(50\bar{5}1)$ < $(40\bar{4}1)$. The activity of the stepped surfaces decreased slightly after oxygen pretreatment of the surface. The results indicated that steps and anion vacancy defects are the active sites for methanol decomposition. The activity of the polar (0001) surface was similar to that of the stepped surfaces. However, the products were different. CD_2O and D_2O, but no CD_4 were observed in addition to CO, CO_2 and D_2. The results indicated that methanol decomposition on ZnO is a structure-sensitive reaction. Implication of these observations on the reverse reaction of methanol synthesis on ZnO and Cu–Zn oxide is discussed.

INTRODUCTION

The concept of structure sensitivity in catalysis was introduced by Boudart (*1*) to classify reactions according to whether the rates per exposed surface atom of the catalyst and other characteristics of the reaction depend on the support, method of preparation, and dispersion. It is believed that these variables ultimately control the electronic properties and the atomic environments of the surface atoms. Since then, many structure-sensitive and structure-insensitive reactions have been reported on supported metal catalysts. While the original concept emphasized on supported catalysts, it has been extending to single-crystal studies in which different crystal planes, some of which possess steps and kinks, exhibit different catalytic behavior (*2–4*). However, practically all studies of the latter type reported to date involved metallic surfaces.

It is conceivable that reactions on oxide catalysts can also be structure-sensitive. Indeed, since most oxide catalysts are prepared by calcination of hydroxide such that the surfaces are formed by dehydroxylation, it has long been proposed that oxide surfaces consist of hydroxyl groups surrounded by different numbers of exposed cations, cations of different numbers of coordinative unsaturation, and oxygen anions (*5, 6*). Different degrees of dehydroxylation generate different ratios of these surface ions and therefore surfaces of different properties. For example, the isomerization and dehydration activities of Al_2O_3 (*7*) and the isomerization activity of Cr_2O_3 (*6*) were found to increase with increasing degree of dehydroxylation. Such observations, which indicated that special surface sites are required for catalysis strongly suggested that these reactions are structure sensitive.

There are other reports that suggested structure sensitivity in oxide catalysis. For

[1] Present address: Central Research and Development Department, E.I. Du Pont de Nemours & Co., Wilmington, Delaware.

[2] To whom all correspondence should be addressed.

0021-9517/83 $3.00

example, the catalytic decomposition of methanol on TiO_2 was found to depend on the crystallographic forms of TiO_2 (*8*). Surface defects have been suggested as the active sites for a number of reactions (*9, 10*).

There has yet to be a report on the study of the catalytic activity of different crystal planes of an oxide. Some chemical properties of single-crystal oxide surfaces have been reported for TiO_2, $SrTiO_3$, and ZnO (*11–13*). In general, it was shown that anion vacancies are chemically more active than the stoichiometric surfaces. For example, water and oxygen adsorb readily on these vacancies.

In addition to anion vacancy defects, structural defects such as surface steps can also be present on oxide surfaces. Recently, the CO, O_2, and CO_2 chemisorption properties have been compared among ZnO surfaces that were perfect and those that contained anion vacancy defects or step defects (*13*). It was found that nonpolar surfaces with steps in the positive *c* direction (Fig. 1) behave like a nonpolar surface with anion vacancies in CO_2 adsorption, but they behave like the Zn-polar surface in CO adsorption. In this report, the reactivity of these surfaces in methanol decomposition are compared. From the reactivity and the product distribution measurements, information on the structure sensitivity of this reaction is obtained. Since methanol decomposition and methanol synthesis are related by the principle of microscopic reversibility, such information should be applicable to the synthesis reaction.

Specifically, the technique of temperature-programmed decomposition spectroscopy (TPDS) was used to study four ZnO surfaces: a nonpolar $(10\bar{1}0)$ surface (the horizontal surface in Fig. 1 if the step were not present), a stepped $(50\bar{5}1)$ and $(40\bar{4}1)$ surface which are surfaces with $(10\bar{1}0)$ terraces and (0001) steps (surface shown in Fig. 1), and a Zn-polar surface (the vertical surface on the right in Fig. 1). The $(40\bar{4}1)$ and the $(50\bar{5}1)$ surfaces can also be labeled $4(10\bar{1}0) \times (0001)$ and $5(10\bar{1}0) \times (0001)$, respectively, and 25 and 20% of their surfaces are steps. The reactivity in methanol decomposition of these surfaces will be described in this paper. The reaction mechanism will be discussed in a later paper.

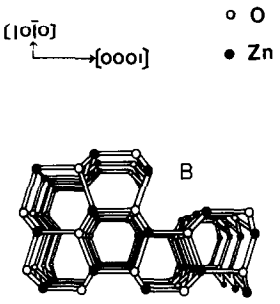

FIG. 1. Model of a stepped nonpolar ZnO surface.

EXPERIMENTAL

Experiments were conducted in a conventional ultra-high vacuum stainless-steel chamber equipped with Auger and LEED optics and a UTI quadrupole mass spectrometer as described elsewhere (*13, 14*). Zinc oxide single crystals were insulating samples purchased from Atomergic Chemicals. The crystal face being studied was 6×6 mm^2. The crystals were oriented by X-ray Laue back-scattering to within 0.5°. The direction of the *c*-axis was determined by etching. The $(40\bar{4}1)$ and the $(50\bar{5}1)$ surfaces were obtained by cutting the crystal at 7.7° and 6.2°, respectively, with respect to the $(10\bar{1}0)$ plane in the direction of positive *c*-axis. The samples were mechanically polished until free of observable scratches under an optical microscope. A thin layer of gold was deposited on the edge and the back side of the samples. The samples were heated by radiation from a tungsten filament.

The surfaces were cleaned and ordered by repeated cycles of sputtering and annealing. The $(10\bar{1}0)$ and the (0001) surfaces were annealed at 500°C for 60 min each time, and the $(40\bar{4}1)$ and $(50\bar{5}1)$ surfaces were annealed first at 650°C for 30 min, and

then at 500°C for 20 min. Details of the preparation have been reported (*13, 14*).

Potassium was the only detectable impurity and the Auger K/O peak ratio was kept below 5%, usually less than 2%. TPRS results were identical on surfaces with and without detectable K.

Sample pretreatment conditions were chosen based on the work of Göpel (*15–17*). By performing studies on ZnO powder and single-crystal ($10\bar{1}0$) plane using techniques such as EPR, surface conductivity, surface potential, and temperature programmed desorption of isotopically labeled oxygen, Göpel and coworkers found that because of preferential vaporization of oxygen, anion vacancies are present on ZnO surfaces that are heated *in vacuo* above 800°K. Exposure of such surfaces at room temperature to oxygen removes these vacancies and results in chemisorbed O_2^- species. The latter chemisorbed species can be desorbed at 350°C leaving behind a stoichiometric surface.

In this study, a surface that was sputtered and annealed as described earlier is referred to as a reduced surface because it contained surface anion vacancies. If a reduced surface was exposed to 1.3×10^{-4} Pa of oxygen at 400°C for 15 min, cooled in O_2 to 200°C, and then *in vacuo* to room temperature, the resulting surface is referred to as an oxidized surface. If the surface was further heated to 350°C *in vacuo* and cooled back to room temperature, it is referred to as a stoichiometric surface. If unspecified; the surface is a reduced surface.

Methanol-d_4 (Chemalog 99.5% enriched) was dosed directly onto the sample surface via a leak valve and a 1/16-in.-o.d. stainless-steel doser in a manner similar to that of Madix (*18*). It was purified by fractional distillation using dry-ice–acetone as refrigerant, and by several freeze-thaw cycles. During dosing, the methanol was kept at 0°C.

The standard procedure for adsorption and desorption was to cool the ZnO sample *in vacuo* ($\sim 10^{-8}$ Pa) for 1 to 1½ h since the last desorption or annealing. Then with the sample facing the doser, methanol was introduced for 15 s. The magnitude of the desorption peaks remained constant for exposures longer than about 5 s. The pressure recorded by the nude ion gauge was 2.7×10^{-7} Pa during exposure, although the effective pressure at the sample surface was much higher. After evacuating the chamber for 2 min, desorption began. The desorbed species was detected by the mass spectrometer which was controlled by a microprocessor such that intensities of 5 masses could be recorded every second. Partial discrimination between desorption signal and the background was achieved by placing a stainless-steel plate with a 1-cm-diameter hole between the sample and the mass spectrometer. A heating rate of 10°C/s was maintained up to 400°C. Between 400 and 550°C, the rate slowed to about 8°C/s.

During thermal desorption, mass numbers corresponding to the parent peaks for CO, CO_2, and D_2, and the various cracked fragments of CD_3OD, CD_2O, D_2O, and CD_4 were monitored. To convert the peak intensities into relative concentrations of the various compounds, the intensities were first corrected for contributions as cracked fragments from the appropriate species, and then corrected for the relative sensitivities of the species. The parent peaks of CO, CO_2, and D_2 were used for such concentration calculations. For methanol, the CD_3O peak ($m/e = 34$) was used, and for formaldehyde, the CDO peak ($m/e = 30$). The cracking patterns for all the above species were independently measured in our system by leaking in the appropriate gas. The identification of the various species were relatively straightforward except for what we assigned as CD_4. Both CD_4 and D_2O have mass 20, but they were distinguished by their cracking patterns at $m/e = 16$ and 14. Specifically, the cracking pattern for CD_4 was $m/e = 20$, 100; 18, 75.4; 16, 14.7; 14, 10.2; 12, 3.3. That for D_2O was difficult to obtain due to H–D exchange in the mass spectrometer. However, it is expected from

the cracking pattern of H_2O that the m/e = 16 fragment (O^+) to be very small, and m/e = 14 fragment to be nonexistent. Thus the m/e = 16 and 14 intensities can be used for CD_4 identification. In the experiments using the stepped surfaces, for example, the peak area ratios for m/e = 20:16:14 is 1:0.21:0.12 (after subtracting contribution from CD_3OD). Within experimental error, the ratios were the same as the ratios in CD_4 cracking pattern. Therefore, the peak was assigned totally to CD_4, and none to D_2O. This assignment was further confirmed by results from similar experiments using CH_3OH instead of CD_3OD. Then the methane formed was CH_4 whose parent peak was m/e = 16 which was clearly distinguishable from H_2O (m/e = 18). The absence of detectable m/e = 18 peak above background desorption confirmed the assignment.

The sensitivity of the mass spectrometer for each species was determined by monitoring the mass spectrometer intensities as a function of pressure determined by the ion gauge which was further corrected for the ionization cross section of the gas. The sensitivity thus determined for CO, CO_2 and O_2 were within 8%. That for D_2 was 2.74 times lower. According to the manufacturer, the mass spectrometer sensitivity for different gases is about the same; we have therefore assumed constant sensitivity for all species except D_2. Because of the low sensitivity for D_2, a small D_2 peak could easily be missed. In addition, the small D_2 signals were more subjected to a constant error in background subtraction, and lower signal to noise than other species. Thus the deuterium balance was less accurate than carbon or oxygen balance.

The peak intensities reported in the tables and figures have all been corrected for contribution from cracking of other species and difference in relative sensitivities.

Peak temperatures in the desorption profiles were reproducible to within 10°K from run to run. Peak intensities were reproducible to within 15%. Data on $(10\bar{1}0)$ surface have been repeated on two different surfaces of different samples. Data on (0001) surface have been repeated on two surfaces prepared from the same crystal, while data on the stepped surfaces were obtained only on one surface each.

In this paper, peak intensities are reported as areas under the desorption peaks. It was found that if the sample was not directly facing the mass spectrometer, the intensities of the desorption peaks decreased uniformly by 70–50%, except for D_2. Because of the uniform behavior of the peaks, the relative peak intensities should reflect the relative concentrations even though we did not separate the contribution due to direct flux from that due to the background pressure increase.

RESULTS

LEED evidence for ordered surfaces after sputtering and annealing cycles has been presented (*13*). Summarizing the results, the $(10\bar{1}0)$ surface exhibited a sharp 1 × 1 pattern. The (0001) surface exhibited a sharp sixfold "1 × 1" pattern which was interpreted as due to the presence of single double-layer steps (*19*). The stepped $(40\bar{4}1)$ and $(50\bar{5}1)$ surfaces exhibited characteristic splitting of spots. Results from the analysis of the characteristic voltages at which the spots became singlets or equal intensity doublets were consistent with the conclusion that there is little relaxation of the surface atoms from positions derived from truncation of an ideal solid. Thus the model shown in Fig. 1 appears to represent well the real surface.

Figure 2 shows the temperature programmed desorption profile of methanol from a $(50\bar{5}1)$ surface. Undissociated methanol was desorbed with a peak maximum at 150°C. Deuterated methane was evolved simultaneously. Between 300 to 450°C, the other products CO, CO_2, and D_2 were desorbed. The peak maxima of CO and D_2 were both at 380°C, and that of CO_2 was at a slightly higher temperature of 400°C. Formaldehyde, methyl formate, and dimethyl-

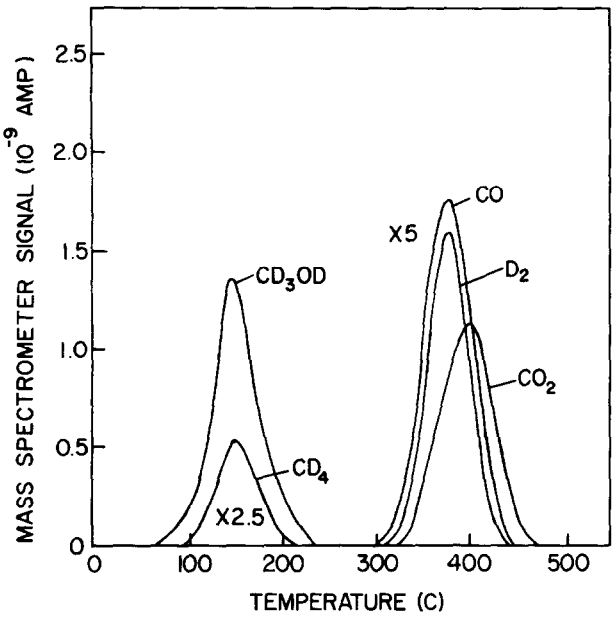

FIG. 2. Temperature-programmed decomposition profile of CD_3OD on a reduced $(50\bar{5}1)$ surface. CD_4 peak was expanded 2.5 times, CO, CO_2, and D_2 5 times.

ether were searched for but not found. Water was not detected. However, because of the relatively large uncertainty in our method of mass analysis as described above, if a small amount of D_2O was evolved together with CD_4, it would not be detected. The assignment of the peak to CD_4 instead of D_2O was described in the last section and confirmed by studying desorption of CH_3OH instead of CD_3OD.

The desorption profiles for the $(40\bar{4}1)$ and the reduced $(10\bar{1}0)$ surfaces are similar to the $(50\bar{5}1)$ surface except for differences in absolute peak intensities on the different surfaces. Within uncertainties, the relative peak areas of the decomposition products were the same on all three surfaces. The area of the CD_3OD peak for the $(10\bar{1}0)$ surface was about 20% higher than for the stepped surfaces. This difference was not considered significant considering the uncontrolled variables involved when comparing different samples, such as precise location of the sample, and performance of the mass spectrometer. The intensities of the decomposed products relative to CD_3OD for each sample would be free of these uncertainties. These ratios for the four products are shown in Fig. 3 and listed in Table 1. The fraction of desorption being decomposition products decreased in the order $(40\bar{4}1)$ > $(50\bar{5}1)$ > reduced $(10\bar{1}0)$ > stoichiometric $(10\bar{1}0)$. The amount of CD_3OD desorbed from the stoichiometric

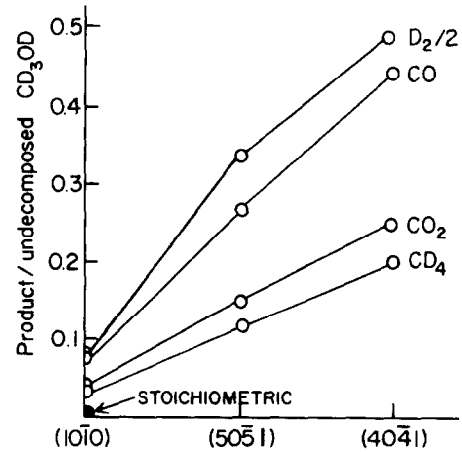

FIG. 3. Ratios of the intensities of the decomposed products to that of CD_3OD for different ZnO surfaces.

TABLE 1

Product Distribution in CD_3OD Decomposition[a]

Surface	CD_3OD	CO_2	CO	CD_4	D_2[b]
$(10\bar{1}0)$	1.00	0.04	0.07	0.036	0.14
$(50\bar{5}1)$	1.00	0.15	0.27	0.12	0.66
$(40\bar{4}1)$	1.00	0.25	0.44	0.20	0.96

[a] These are peak areas normalized to CD_3OD (measured as CD_3O, m/e = 34).

[b] These values are D_2 peak areas times 2.74, the mass spectrometer sensitivity factor.

$(10\bar{1}0)$ surface was about 25–30% lower than the reduced $(10\bar{1}0)$, while the decomposed products were barely detectable. Referring to data in Table 1, it is interesting to note that the ratio of CD_4/CO_2 is close to unity.

Methanol decomposition was also studied on a stoichiometric and an oxidized $(40\bar{4}1)$ surface defined and pretreated as described in the experimental section. The amounts of decomposition products relative to CD_3OD are listed in Table 2 and compared with a reduced $(40\bar{4}1)$ surface. A heating rate of 5°K s^{-1} was used for these experiments instead of the usual 10°K s^{-1}. Within experimental uncertainties, the product distribution of decomposition products seemed to be about the same on the three surfaces, although the fraction of methanol decomposed might be slightly larger on the reduced surface.

The desorption profile for the Zn-polar (0001) surface, which is shown in Fig. 4 was markedly different from those for the other surfaces. Three D_2 and CO peaks were observed. CD_4 was not found. Instead, small CD_2O and D_2O peaks were observed. The relative peak areas of these products are shown in Table 3. Comparing with the data in Table 1, it can be seen that the fraction of desorbed products being decomposition products was higher on this surface than on the other surfaces. Table 3 also shows the product distributions as a function of the annealing temperature of its surface. It was reported that annealing between 300 and 400°C resulted in a (0001) surface that exhibited splitting of the spots of the sixfold 1 × 1 pattern (*13*). This suggested the formation of regular steps on the surface. Annealing between 500 and 600°C resulted in a sharp sixfold 1 × 1 pattern (*13*). The data in Table 3 show that the (0001) surface under these different conditions gave similar product distributions in methanol decomposition.

The surface coverages of methanol were estimated from the desorption peak areas in experiments where the sample was not facing the mass spectrometer. In this manner, the mass spectrometer measured the partial pressure of the individual gas in the chamber. From the known pumping speed of the gases, the number of molecules desorbed and therefore the surface coverage can be calculated. These coverage values are shown in Table 4.

DISCUSSION

Two interesting observations were made here. First, it was shown that the reactivity of the surfaces for methanol decomposition depended markedly on the detailed atomic structure of the surface. Second, the Zn-polar plane showed a completely different product distribution as compared to the other surfaces.

Since the total surface coverage of methanol on the different surfaces was compara-

TABLE 2

Product Distribution in CD_3OD Decomposition on Different $(40\bar{4}1)$ Surfaces[a]

Surface	CD_3OD	CO_2	CO	CD_4	D_2[b]
Oxidized	1.00	0.29	0.32	0.17	0.79
Stoichiometric	1.00	0.24	0.30	0.17	[c]
Reduced	1.00	0.30	0.41	0.18	1.15

[a] These are peak areas normalized to CD_3OD (measured as CD_3O, m/e = 34). Sample heating rate was 5°C s^{-1}.

[b] These are D_2 peak areas times 2.74, the mass spectrometer sensitivity factor.

[c] Not measured.

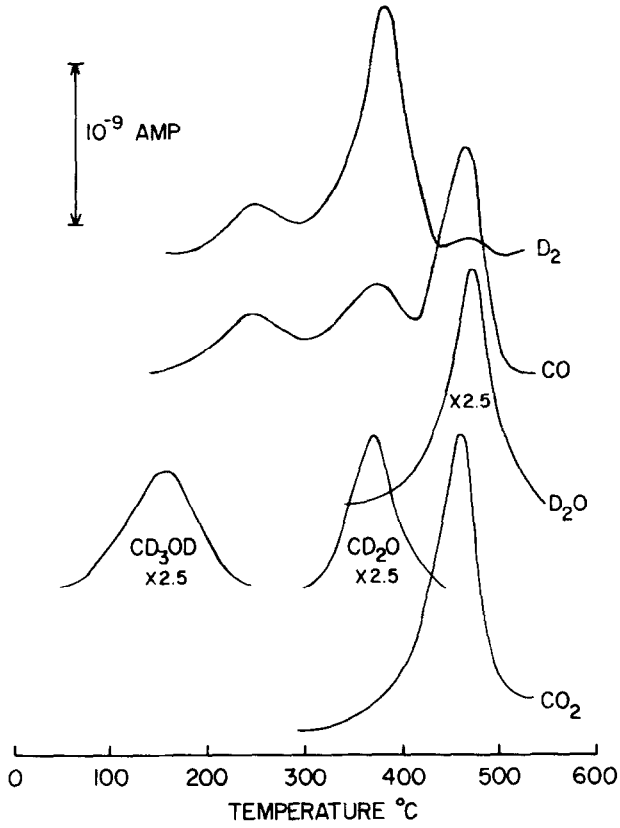

FIG. 4. Temperature-programmed decomposition profile of CD_3OD on a (0001) surface.

ble (Table 4), results in Tables 1 and 3 showed that the polar (0001) surface and the stepped nonpolar surfaces are comparable in methanol decomposition activity. While the percentage of adsorbed methanol decomposed on the polar plane was the highest, some of the products were evolved only at very high temperature suggesting that they were produced by a pathway of high activation energy. Therefore, quantitative comparison of the methanol decomposition reactivity between the polar and the

TABLE 3

Product Distribution in CD_3OD Decomposition on (0001) Surface[a]

Annealing temp.[b] (°C)	CO_2	CO			CD_3OD	CD_2O	D_2O	D_2[c]	
		260°C	360°C	450°C				260°C	360°C
385	3.14	1.33	1.01	2.26	1.00	1.05	1.19	2.41	6.30
500	3.36	1.49	1.42	2.10	1.00	1.00	1.16	2.85	7.12
600	3.31	1.57	1.02	2.48	1.00	0.82	1.22	[d]	6.55

[a] These are peak areas normalized to CD_3OD (measured as CD_3O, $m/e = 34$).
[b] The (0001) surface was annealed *in vacuo* at these temperatures before experiment.
[c] These are D_2 peak areas times 2.74, the mass spectrometer sensitivity factor.
[d] Not measured.

TABLE 4

Surface Coverage of Methanol on Different Surfaces[a]

Surface	Coverage[b] (10^{-2})
$(10\bar{1}0)$	0.81
$(50\bar{5}1)$	0.82
(0001)	1.12

[a] The coverage was calculated using a pumping speed of 80 liters s^{-1}, and a mass spectrometer sensitivity of 12.6 A/Torr. One monolayer of coverage is taken as 6×10^{14} molecules/cm^2.

[b] These are the coverages of methanol immediately before temperature-programmed desorption.

stepped surfaces cannot be made without knowledge of the activation energies. Ordering of the reactivity of the other surfaces is readily obtained as $(40\bar{4}1) > (50\bar{5}1) >$ reduced $(10\bar{1}0) >$ stoichiometric $(10\bar{1}0)$.

There are several factors that could contribute to the relatively high reactivity of the polar surface. An unreconstructed polar surface has a layer of Zn ions slightly more outward than a layer of O ions. This results in a strong outward pointing dipole moment which would result in strong interaction between the surface and molecules that possess dipole moments, such as methanol. Another consequence is that the surface would have high surface energy which causes the surface to reconstruct readily. Indeed, the least complicated LEED pattern observable on a polar surface is the sixfold 1×1 pattern (*20, 21*) which has been explained by the presence of one double-layer step (*19*). Splitting of the LEED spots were readily observed on cleaved (*22*) and sputtered-annealed surfaces (*13, 23*). This is attributed to the presence of regular two double-layer steps. More complicated (5×1), (2×2), $(4\sqrt{3} \times 4\sqrt{3} - 30°)$, and (3×3) reconstructions have all been reported (*21, 24*). These patterns indicated reconstruction into other well-ordered surfaces that has coherent length large enough for low-energy electron diffraction. There may well be other lower density and less regular defects present that are not detected by the simple LEED detection on the phorescent screen. Therefore, it may be concluded that the polar surface is normally a surface of a rather high density of defects. If some of these defects are active in methanol decomposition, it could explain the high activity of this surface. Among the possible types of reconstruction, the regular two double-layer steps are probably inactive in methanol decomposition. This follows from the observation of Table 3 which shows that a polar surface preannealed to 350°C so as to develop split LEED spots showed the same methanol decomposition activity as the surface preannealed to higher temperatures and showed only sharp sixfold 1×1 patterns.

Finally, the product distribution observed for the polar surface suggests that the mechanism of methanol decomposition on this surface is different from that on other surfaces. Different mechanisms could proceed at different rates. As mentioned earlier, discussion of the reaction mechanisms will be deferred to a later publication.

The product distributions for the stepped and the flat nonpolar surfaces are identical. Thus the decomposition proceeds via identical mechanism on these surfaces. The ordering in reactivity for these surfaces must therefore reflect the ordering in active site density. It is interesting that this ordering parallels the defect densities. The $(40\bar{4}1)$ surface which has on the average 25% of the surface being steps is the most active, the $(50\bar{5}1)$ which has 20% of the surface being steps is second, the reduced $(10\bar{1}0)$ which has anion vacancies but no steps is third, and the stoichiometric $(10\bar{1}0)$ is the least active. This observation strongly suggests that on these surfaces the active site must be associated with anion vacancies or step defects. Furthermore, it suggests that the step defects behave like anion vacan-

cies in this reaction. This is not totally surprising if the diagram in Fig. 1 realistically models the stepped surface. From the diagram, it can be seen that when a molecule approaches the step, it would interact with the two coordinatively unsaturated bonds of the two zinc ions, one above and one below the step. On the other hand, a molecule approaching a surface anion vacancy would interact with the coordinatively unsaturated bonds of the surrounding three zinc ions, while a molecule approaching a stoichiometric surface would interact with one zinc ion. Thus the local environment of a step site is closer to an anion vacancy than a site on the terrace. Furthermore, the vertical section of the step can also be viewed as a small fraction of the polar (0001) surface. The strong dipole moment present there should also enhance the strength of interaction of the site with methanol.

A question can be raised as to whether the step sites themselves directly account for the enhanced reactivity of the stepped surface as compared to the flat surface, or whether the presence of steps stabilizes a higher density of point anion vacancies on the terrace which are the true active sites. Data in Table 2 tend to discount the latter possibility. It was found that the reactivity of the stepped surface only decreased slightly after the surface was pretreated with oxygen in a procedure that significantly removes anion vacancies on the prismatic surface. The anion vacancies on the $(10\bar{1}0)$ terraces should behave like the $(10\bar{1}0)$ plane. Thus the results suggest that the step sites account for most of the reactivity with only minor contribution from anion vacancies on the terraces.

The results here also demonstrated that single-crystal studies can greatly supplement studies using powder catalysts. In a recent study of methanol decomposition on ZnO powder using temperature-programmed decomposition spectroscopy technique (*25*), a ZnO powder was used which was prepared by ignition of zinc in an oxidizing atmosphere and showed a ratio of exposed areas of the prismatic $(10\bar{1}0)$ face to polar (0001) and $(000\bar{1})$ face of about 6 : 1 as determined by transmission electron microscopy. Comparing their desorption data with those reported here, it is found that the product distribution and the order of appearance of the products showed marked resemblance between their results and those observed here on the (0001) plane. It appears that although the Zn-polar surface is only present as a minor surface on their ZnO powder, it accounted for the observed methanol decomposition activity. This can be readily understood from our results because defects of anion vacancies or steps are needed for reactivity on the prismatic plane. The density of such defects on their powder might be low because of the particular method of preparation, and because their catalyst was not heated to higher than 700°K in their experiments.

One more difference between the polar and the nonpolar surfaces should be mentioned. The appearance of formaldehyde on the (0001) surface suggests that the surface possesses a higher dehydrogenation activity than the stepped or the nonpolar surfaces. It suggests that the (0001) surface is more metallic in nature. This point will be further discussed in a future publication.

Although methanol decomposition was studied with TPDS one may assume that the steady-state reactivity parallels the reactivity observed here. Thus the polar and the stepped surfaces are expected to be rather active in steady-state catalytic methanol decomposition. A reduced nonpolar $(10\bar{1}0)$ surface will have some activity, and a stoichiometric $(10\bar{1}0)$ surface will be almost inactive. Since methanol decomposition and methanol synthesis are related by the principle of microscopic reversibility, it can be concluded that an active ZnO methanol synthesis catalyst should contain mostly Zn polar planes and stepped nonpolar planes. Other planes and defects may also be active, but such information is not provided from this study.

The catalyst for low-temperature methanol synthesis from syngas is based on Cu–Zn oxide. It has been shown that on varying the Cu/Zn ratio, two activity maxima were observed (*26*). Electron microscopy investigation of the two catalysts corresponding to the maxima indicated that in one catalyst, the oxide appeared to be long needles of hexagonal cross sections, and in the other catalyst, thin hexagonal platelets. The active component of the catalyst was proposed to be a solid solution of Cu(I) in ZnO (*26–28*) where the function of Cu(I) is to activate carbon monoxide. The majority of the exposed surface of the needle-shaped crystallites is the nonpolar plane, while that of the hexagonal platelet crystallites is the polar plane. It is interesting that the two types of crystallites are both highly active. In view of the results here, it is not surprising that the hexagonal platelets are highly active. On the other hand, the high activity of the needle-shaped crystallites may indicate the presence of a high density of surface defects, in particular anion vacancies. Therefore, it is possible that the function of Cu(I) is, in addition to activating carbon monoxide, to generate and stabilize anion vacancies through charge balance in the crystallite, as has been proposed earlier (*10*).

CONCLUSION

Methanol decomposition on ZnO has been shown to be a structure-sensitive reaction. The activity and the reaction mechanism depend on the detailed atomic environment of the surface. The Zn polar surface is active in the reaction. The nonpolar surface requires the presence of defects to be active, such as steps and anion vacancies. The reactivity depends on the defect density.

ACKNOWLEDGMENT

This work was supported by the Department of Energy, Basic Energy Sciences Division. WHC acknowledges support by the Materials Research Center of Northwestern University from 1977–1981.

REFERENCES

1. Boudart, M., *Adv. Catal.* **20,** 153 (1969).
2. Somorjai, G. A., *in* "Chemistry in Two Dimensions: Surfaces." Cornell Univ. Press, 1981.
3. Somorjai, C. A., *Acc. Chem. Res.* **9,** 248 (1976).
4. Ertl, G., *Catal. Rev.* **21,** 201 (1980).
5. Peri, J. B., *J. Phys. Chem.* **69,** 220 (1965).
6. Burwell, R. L., Jr., Haller, G. L., Taylor, K. C., and Reed, J. F., *Adv. Catal.* **20,** 1 (1969).
7. Pines, H., and Manassen, J., *Adv. Catal.* **16,** 49 (1966).
8. Carrizosa, I., Muneura, G., and Castanar, S., *J. Catal.* **49,** 265 (1977).
9. Knozinger, H., and Ratnasamy, P., *Catal. Rev.* **17,** 31 (1978).
10. Kung, H., *Catal. Rev.* **22,** 235 (1980).
11. Henrich, V. E., *Prog. Surf. Sci.* **9,** 143 (1979).
12. Göpel, W., Bauer, R. S., and Hansson, G., *Surf. Sci.* **99,** 138 (1980).
13. Cheng, W. H., and Kung, H. H., *Surf. Sci.* **122,** 21 (1982).
14. Cheng, W. H., Ph.D. thesis, Northwestern University, 1982.
15. Göpel, W., Brillson, L. J., and Brucker, C. F., *J. Vac. Sci. Technol.* **17,** 894 (1980).
16. Göpel, W., *Surf. Sci.* **62,** 165 (1977).
17. Runge, F., and Göpel, W., *Z. Phys. Chem. Neue Forge* **123,** 173 (1980).
18. McCarthy, J., Falconer, J., and Madix, R. J., *J. Catal.* **30,** 235 (1973).
19. Henrich, V. E., Zeiger, H. J., Solomon, E. I., and Gay, R. R., *Surf. Sci.* **74,** 682 (1978).
20. Levine, J. D., Willis, H., Bottons, W., and Mark, P., *Surf. Sci.* **29,** 144 (1972).
21. Chang, S. C., and Mark, P., *Surf. Sci.* **46,** 293 (1974).
22. Henzler, M., *Surf. Sci.* **36,** 109 (1973).
23. Gay, R., Nudine, M., Henrich, V., Zeiger, H., and Solomon, E., *J. Amer. Chem. Soc.* **102,** 6752 (1980).
24. Fiermans, L., Arijs, E., Vennik, J., and der Vorst, W., *Surf. Sci.* **39,** 357 (1973).
25. Bowker, M., Houghton, H., and Waugh, K. C., *J. Chem. Soc. Faraday Trans. 1,* **77,** 3023 (1981).
26. Herman, R. G., Klier, K., Simmons, G. W., Finn, J. B., Bulko, J. B., and Kobylinski, T. P., *J. Catal.* **56,** 407 (1979).
27. Bulko, J. B., Herman, R. G., Klier, K., and Simmons, G. W., *J. Phys. Chem.* **83,** 3118 (1979).
28. Mehta, S., Simmons, G. W., Klier, K., and Herman, R. G., *J. Catal.* **57,** 339 (1979).